

Dynamical origin of shear flow induced modifications of magnetic islands

This article has been downloaded from IOPscience. Please scroll down to see the full text article.

2007 Nucl. Fusion 47 1238

(<http://iopscience.iop.org/0029-5515/47/9/021>)

View [the table of contents for this issue](#), or go to the [journal homepage](#) for more

Download details:

IP Address: 122.179.52.180

The article was downloaded on 22/02/2011 at 10:28

Please note that [terms and conditions apply](#).

Dynamical origin of shear flow induced modifications of magnetic islands

D. Chandra, A. Sen and P. Kaw

Institute for Plasma Research, Bhat, Gandhinagar 382428, India

Received 5 January 2007, accepted for publication 10 July 2007

Published 29 August 2007

Online at stacks.iop.org/NF/47/1238

Abstract

A generalized Newcomb equation that incorporates inertial contributions from equilibrium shear flows as well as finite β contributions is derived in a cylindrical geometry. It is shown from numerical solutions of this equation that the stability parameter Δ' can be significantly influenced by flow as it becomes a sensitive function of the global profiles of the magnetic field and flow velocity. These results can have important implications for the nonlinear evolution of magnetic islands in the presence of flows.

PACS numbers: 52.55Fa, 52.55Tn, 52.35Py, 52.65kj

(Some figures in this article are in colour only in the electronic version)

1. Introduction

The nonlinear evolution of magnetic islands due to unstable classical or neoclassical tearing modes is a topic of much current interest particularly in the context of confinement limits for long pulse experiments in superconducting tokamaks [1]. The size and lifetimes of these magnetic islands set a limit on the plasma β and are an important concern for future reactor configurations. Much attention is therefore being directed towards the experimental and theoretical elucidation of factors that affect the onset and saturation of such islands. The Rutherford theory of neoclassical tearing modes has provided a particularly useful analytical paradigm for understanding the nonlinear behaviour of the islands and has also been the basis for the formulation of various stabilization schemes [2]. Large scale numerical simulation initiatives, such as NIMROD [3], involving a direct solution of model MHD equations constitute an alternative and complementary approach to this problem. An important issue that has not yet been satisfactorily resolved and needs detailed exploration relates to the dynamical interaction of the magnetic islands with equilibrium shear flows. Flows are ubiquitous in most tokamak plasmas and can arise from a variety of causes such as unbalanced neutral beam injection, radio frequency heating or as a by-product of micro-turbulence. Some of the basic issues related to the influence of sheared flows on resistive instabilities have been known for a long time and have been investigated in simplified geometries and model flow profiles in several past studies [4–7]. In other related works the combined influence of a resistive wall and a rigid plasma rotation on the stability of kink modes, tearing modes and resistive wall modes has been examined [8, 9]. However the detailed assessment

of sheared flow effects on magnetic island dynamics for realistic geometries either through an analytic approach or by means of numerical simulations poses serious mathematical as well as computational challenges. Some recent attempts in this direction, e.g. numerical investigations employing a fully toroidal code [10] based on generalized reduced MHD equations [11] have revealed a number of interesting results. It has been found, for example, that differential flow provides a strong stabilizing influence leading to lower saturated island widths for the classical tearing mode and reduced growth rates for the neoclassical tearing mode. The effect of velocity shear is found to depend on the sign of the shear at the mode resonant surface with the negative shear providing a destabilizing effect and the positive shear acting in a stabilizing fashion [10, 12]. These results have been found for toroidal sheared flows that are restricted in magnitude to be a fraction of the Alfvén velocity and for equilibrium plasmas that have a small inverse aspect ratio ($R/a \sim 10$, where a and R are the minor and the major radii, respectively). While some general qualitative features of these numerical results can be identified from selective switching on and off of various terms of the model equations a detailed analytic understanding of the dynamical origin of many of the flow induced physical effects is still lacking.

In this paper we discuss an important flow induced effect that can significantly alter the general Rutherford model results. In the present applications of the Rutherford model for neoclassical tearing modes one generally adopts the standard value of the stability parameter Δ' that is given by the linear stability theory of tearing modes in a slab geometry. The value of Δ' can significantly change due to finite β effects [13] and curvature induced effects in the perturbed parallel current

density [14]. Apart from these static equilibrium effects, some past studies [5,7] have also pointed out that equilibrium sheared flows can influence the value of Δ' . However, such studies have been restricted to some simple cases such as poloidal flows and zero β plasmas. Here we derive a generalized version of the outer layer equations in a cylindrical geometry that incorporates both inertial contributions of flow and finite β terms and show through numerical solutions that the value of Δ' can be significantly influenced by the combination of the velocity and magnetic field profiles. Our findings should prove useful in extending the applicability of the Rutherford model and also in the interpretation of numerical investigations carried out on more complex codes such as NIMROD. Based on our understanding of these flow induced effects one can hope to develop experimental strategies that can exploit flows for mitigation or a better control of island growths in long pulsed tokamak experiments.

2. Newcomb equation in the presence of flow

We consider a uniform density incompressible plasma in a cylindrical geometry (r, θ, z) that has a uniform equilibrium flow along the z axis and a sheared poloidal flow along the θ direction. To describe the outer layer dynamics we consider the ideal MHD model equations given by

$$\rho \left[\frac{\partial \mathbf{V}}{\partial t} + (\mathbf{V} \cdot \nabla) \mathbf{V} \right] = -\nabla P + \mathbf{J} \times \mathbf{B}, \quad (1)$$

$$\mathbf{E} + \mathbf{V} \times \mathbf{B} = 0, \quad (2)$$

$$\nabla \times \mathbf{B} = \mu_0 \mathbf{J}; \quad \nabla \times \mathbf{E} = -\frac{\partial \mathbf{B}}{\partial t}, \quad (3)$$

$$\nabla \cdot \mathbf{B} = 0; \quad \nabla \cdot \mathbf{V} = 0. \quad (4)$$

We assume the equilibrium quantities to be of the form

$$\mathbf{B}_0 = B_{0\theta}(r)\hat{\boldsymbol{\theta}} + B_{0z}(r)\hat{\boldsymbol{z}}; \quad \mathbf{V}_0 = V_{0\theta}(r)\hat{\boldsymbol{\theta}} + V_{0z}(r)\hat{\boldsymbol{z}}. \quad (5)$$

The ideal equilibrium, obtained from the momentum equation (1), is then given by the relation

$$\frac{\beta}{2} \frac{dP_0}{dr} = \frac{V_{0\theta}^2}{r} - \frac{B_{0\theta}^2}{r} - B_{0\theta} \frac{dB_{0\theta}}{dr} - B_{0z} \frac{dB_{0z}}{dr}, \quad (6)$$

where we have normalized the magnetic field by B_{0z} , the velocity field by $V_A (= B_{0z}/(\mu_0 \rho_0)^{1/2})$ and pressure by $P_{00} = \beta B_{0z}^2/2\mu_0$. Here P_{00} and B_{0z} are the peak values of the pressure and the axial magnetic field respectively (with the peaks assumed to occur at the magnetic axis) and $\beta = 2\mu_0 P_{00}/B_{0z}^2$.

We next linearize equations (1) and (2) about these equilibrium quantities and assume the perturbed quantities to have a time dependence of the form $f_1(r, \theta, z, t) = f_1(r, \theta, z) \exp(i\omega t)$. The frequency ω is complex for an unstable tearing mode with the real part denoting the rotation of the island and the imaginary part denoting the growth rate of the mode. We neglect the imaginary part and assume ω to be real. This is appropriate for the ideal external region where resistivity can be neglected and the mode growth term, which scales as some power of the resistivity, is also very small. The perturbed quantities then obey the following set of equations:

$$(i\omega + \mathbf{V}_0 \cdot \nabla) \mathbf{V}_1 + (\mathbf{V}_1 \cdot \nabla) \mathbf{V}_0 = -\nabla p_1^* + (\mathbf{B}_0 \cdot \nabla) \mathbf{B}_1 + (\mathbf{B}_1 \cdot \nabla) \mathbf{B}_0, \quad (7)$$

$$(\mathbf{B}_1 \cdot \nabla) \mathbf{V}_0 - (i\omega + \mathbf{V}_0 \cdot \nabla) \mathbf{B}_1 + (\mathbf{B}_0 \cdot \nabla) \mathbf{V}_1 - (\mathbf{V}_1 \cdot \nabla) \mathbf{B}_0 = 0, \quad (8)$$

where $p_1^* = \frac{\beta}{2} P_1 + \mathbf{B}_0 \cdot \mathbf{B}_1$. We assume the perturbed quantities to have a spatial dependence of the form $f_1(r, \theta, z) = f_1(r) \exp(im\theta + ik_z z)$. We further define

$$\mathbf{F} = \mathbf{k} \cdot \mathbf{B}_0; \quad \tilde{\mathbf{G}} = \mathbf{k} \cdot \mathbf{V}_0,$$

where $\mathbf{k} = (0, m/r, k_z)$. It is also convenient at this point to transform to a rotating frame defined by $\omega = -\tilde{G}(r_s)$ where r_s is the particular mode rational surface of the growing tearing mode [7]. The radial components of equations (7) and (8) then give

$$-F B_{1r} + i \frac{2}{r} (V_{0\theta} V_{1\theta} - B_{0\theta} B_{1\theta}) + G V_{1r} - i \frac{dp_1^*}{dr} = 0, \quad (9)$$

$$V_{1r} = \frac{G}{F} B_{1r}, \quad (10)$$

where $G = \omega + \tilde{G}$. Further, the θ and z components of equations (7) and (8) can be used to obtain the following equations:

$$i p_1^* = \frac{B_{1r}}{r} \left(H \frac{\partial F}{\partial r} + \frac{2m B_{0\theta} H}{r^2} - \frac{H F}{r} \right) - \frac{H F}{r} \frac{\partial B_{1r}}{\partial r} - \frac{V_{1r}}{r} \left(H \frac{\partial G}{\partial r} + \frac{2m V_{0\theta} H}{r^2} - \frac{H G}{r} \right) + \frac{H G}{r} \frac{\partial V_{1r}}{\partial r}, \quad (11)$$

$$i \frac{2}{r} (V_{0\theta} V_{1\theta} - B_{0\theta} B_{1\theta}) = \frac{2m(i p_1^*) (V_{0\theta} G - B_{0\theta} F)}{r^2 (F^2 - G^2)} + \left[\frac{2(F B_{1r} + G V_{1r})}{(F^2 - G^2)} \left(\frac{B_{0\theta}^2}{r^2} + \frac{V_{0\theta}^2}{r^2} \right) - \frac{4V_{0\theta} B_{0\theta}}{r^2} \right. \\ \left. \times \frac{(G B_{1r} + F V_{1r})}{(F^2 - G^2)} - \left(\frac{\partial V_{0\theta}^2}{\partial r} - \frac{\partial B_{0\theta}^2}{\partial r} \right) \left(\frac{F B_{1r}}{r} - \frac{G V_{1r}}{r} \right) \right. \\ \left. + \left(B_{0\theta} \frac{\partial V_{0\theta}}{\partial r} - V_{0\theta} \frac{\partial B_{0\theta}}{\partial r} \right) (G B_{1r} - F V_{1r}) \right], \quad (12)$$

where $H = r^3/(k_z^2 r^2 + m^2)$. Using equations (11) and (12) to substitute for p_1^* and $(V_{0\theta} V_{1\theta} - B_{0\theta} B_{1\theta})$ in equation (9) and after some rearrangement of terms one gets,

$$F \frac{d}{dr} \left(H \frac{d\psi}{dr} \right) - \frac{2mH}{r^2 \alpha} \frac{G}{F} \left(V_{0\theta} - \frac{G}{F} B_{0\theta} \right) \frac{d\psi}{dr} - \psi \frac{d}{dr} \\ \times \left(H \frac{dF}{dr} \right) - F \psi \left[r + \frac{2m}{r^2 F^2 \alpha} \left(H \frac{dF}{dr} + \frac{2m B_{0\theta} H}{r^2} - \frac{H F}{r} \right) \left(B_{0\theta} - \frac{G}{F} V_{0\theta} \right) - \frac{2}{r F^2 \alpha} (B_{0\theta}^2 + V_{0\theta}^2) + \frac{4}{r F^2 \alpha} \right. \\ \left. \times \frac{G}{F} V_{0\theta} B_{0\theta} + \frac{1}{F^2 \alpha} \left(\frac{dV_{0\theta}^2}{dr} - \frac{dB_{0\theta}^2}{dr} \right) + \frac{r}{F} \frac{d}{dr} \left(\frac{2m B_{0\theta} H}{r^3} \right) - \frac{r}{F} \frac{d}{dr} \left(\frac{H F}{r^2} \right) - \frac{H}{r F} \frac{dF}{dr} - r \frac{G}{F} \left(B_{0\theta} \frac{dV_{0\theta}}{dr} - V_{0\theta} \frac{dB_{0\theta}}{dr} \right) \right] \\ = G \frac{d}{dr} \left(H \frac{dW}{dr} \right) - \frac{2mH}{r^2 \alpha} \left(V_{0\theta} - \frac{G}{F} B_{0\theta} \right) \frac{dW}{dr} - W \frac{d}{dr} \left(H \frac{dG}{dr} \right) - G W \left[r + \frac{2m}{r^2 G F \alpha} \left(H \frac{dG}{dr} + \frac{2m V_{0\theta} H}{r^2} - \frac{H G}{r} \right) \left(B_{0\theta} - \frac{G}{F} V_{0\theta} \right) + \frac{2}{r F^2 \alpha} (B_{0\theta}^2 + V_{0\theta}^2) - \frac{4}{r G F \alpha} \right. \\ \left. \times V_{0\theta} B_{0\theta} + \frac{1}{F^2 \alpha} \left(\frac{dV_{0\theta}^2}{dr} - \frac{dB_{0\theta}^2}{dr} \right) + \frac{r}{G} \frac{d}{dr} \left(\frac{2m V_{0\theta} H}{r^3} \right) - \frac{r}{G} \frac{d}{dr} \left(\frac{H G}{r^2} \right) - \frac{H}{r G} \frac{dG}{dr} - r \frac{F}{G} \right. \\ \left. \times \left(B_{0\theta} \frac{dV_{0\theta}}{dr} - V_{0\theta} \frac{dB_{0\theta}}{dr} \right) \right], \quad (13)$$

where $\alpha = 1 - (G^2/F^2)$ and we have simplified the notation somewhat by using ψ for normalized B_{1r} and W for normalized V_{1r} . Further, using equations (6) and (10) in above equation (13) and after affecting some simplifications one can get the following equation in the single variable ψ ,

$$H \frac{d^2 \psi}{dr^2} + \left(\frac{dH}{dr} + h_f \right) \frac{d\psi}{dr} - \left[\frac{g}{F^2} + \frac{g_f}{F^2} + \frac{1}{F} \frac{d}{dr} \left(H \frac{dF}{dr} \right) \right] \psi = 0 \quad (14)$$

where

$$\begin{aligned} g &= \frac{(\alpha m^2 - 1)rF^2}{\alpha(k_z^2 r^2 + m^2)} + \frac{k_z^2 r^2}{\alpha(k_z^2 r^2 + m^2)} \\ &\times \left(\alpha r F^2 + F \frac{2(k_z r - m B_{0\theta})}{k_z^2 r^2 + m^2} + \beta \frac{dP_0}{dr} \right), \\ h_f &= \frac{2HG}{\alpha F} \left(\frac{G}{F} \frac{1}{F} \frac{dF}{dr} - \frac{1}{F} \frac{dG}{dr} \right), \\ g_f &= \frac{2HG}{\alpha F} \frac{dF}{dr} \left(\frac{G}{F} \frac{dF}{dr} - \frac{dG}{dr} \right) + \frac{4}{r\alpha^2} \frac{G}{F} V_{0\theta} B_{0\theta} + \frac{GH}{r\alpha} \\ &\times \left(\frac{\partial G}{\partial r} + \frac{2mV_{0\theta}}{r^2} \right) + \frac{2V_{0\theta}}{\alpha} \frac{dV_{0\theta}}{dr} - \frac{G}{\alpha} \frac{d}{dr} \left(\frac{2mHV_{0\theta}}{r^2} \right) \\ &+ \left(\frac{m^2}{k_z^2 r^2 + m^2} - \frac{2}{\alpha} \right) \frac{2V_{0\theta}^2}{r\alpha} + \frac{Gr}{\alpha} \frac{d}{dr} \left(\frac{HG}{r^2} \right) \\ &+ \left(\frac{4}{\alpha^2} \frac{k_z^2 r^2}{k_z^2 r^2 + m^2} \frac{G}{F} \frac{B_{0\theta}}{r} - \frac{2mH}{r^2 \alpha^2} \left(\frac{dG}{dr} - \frac{G}{r} \right) \right) \\ &\times \left(V_{0\theta} - \frac{G}{F} B_{0\theta} \right) - \left(\frac{2mHG}{r^2 \alpha^2} \frac{dG}{dr} + \frac{2mV_{0\theta}}{r^2} - \frac{G}{r} \right) \\ &\times \left(B_{0\theta} - \frac{G}{F} V_{0\theta} \right). \end{aligned}$$

For $G = 0$ and $\beta = 0$ equation (14) reduces to the standard outer layer equation that has been analysed in the paper by Furth, Rutherford and Selberg [15]. More recently, Nishimura *et al* [13] have extended the results of [15] to include finite β effects and have shown that finite β can have a stabilizing effect on Δ' . The effect of equilibrium sheared flows on Δ' has been examined in the past by Chen and Morrison [5] but only in a simple slab geometry. For G finite and in the limit of a slab geometry ($r \rightarrow \infty, d/dr \rightarrow d/dx$) our equation (14) reduces to the set of equations that have been discussed by Chen and Morrison [5]. Note that in the slab limit the finite β contribution disappears. Thus equation (14) represents a more generalized description of the outer layer dynamics that takes into account finite β contributions, cylindrical curvature effects as well as sheared flow effects.

Equation (14) is singular at the mode rational surface ($r = r_s$) and the solution ψ has a discontinuity in its derivative across this surface. The measure of this discontinuity is given by the parameter Δ' , defined as

$$\Delta' = \frac{1}{\psi(r_s)} \left[\frac{d\psi}{dr}(r_{s+}) - \frac{d\psi}{dr}(r_{s-}) \right], \quad (15)$$

where $r_{s\pm} = r_s \pm \delta$. Multiplying equation (14) by $r\psi$, dividing by H and integrating over the radius in the range of $\{0, r_{s-}\}$

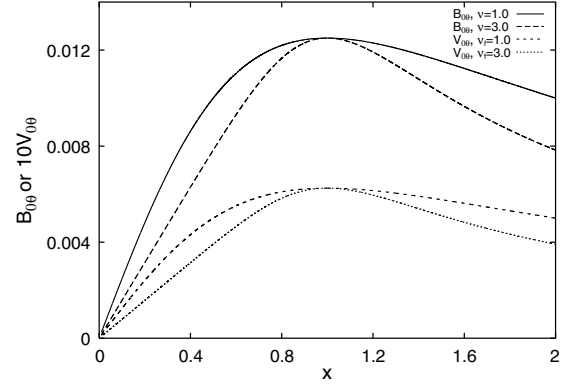


Figure 1. Profiles of $B_{0\theta}$ and $V_{0\theta}$.

and $\{r_{s+}, a\}$ one can obtain the following expression for Δ' ,

$$\begin{aligned} \Delta' &= -\frac{1}{r_s \psi_s^2} \int_0^a \left[\left(\frac{d\psi}{dr} \right)^2 + \left\{ \frac{g}{HF^2} + \frac{1}{HF} \frac{d}{dr} \left(H \frac{dF}{dr} \right) \right. \right. \\ &\quad \left. \left. - \frac{2m^2 k_z^2}{(k_z^2 r^2 + m^2)^2} + \frac{g_f}{HF^2} + \frac{1}{2r} \frac{d}{dr} \left(\frac{r h_f}{H} \right) \right\} \psi^2 \right] r dr. \end{aligned} \quad (16)$$

In arriving at the above expression we have assumed the usual boundary conditions for the mode to be $\psi(a) = 0$ (conducting outer boundary wall) and $\psi(r) \sim r^m, m > 0$ as $r \rightarrow 0$. The various terms in the integral can be identified with physical energy contributions from various quantities such as the magnetic perturbation, velocity perturbation and equilibrium flows. Since the expression involves gradients of equilibrium quantities such as the flow and the magnetic field, their profiles can play an important role in determining the sign and magnitude of Δ' . The profile dependence can be quite sensitive due to the predominance of contributions from terms which become singular near the mode rational surface where $F \rightarrow 0$. The variation of Δ' with various equilibrium parameters is the principal subject of our numerical investigations presented in the subsequent sections.

3. Numerical evaluation of Δ'

To investigate the influence of flows on the outer layer dynamics we have solved equation (14) numerically to determine Δ' for a model set of profiles of $B_{0\theta}$ and velocity $V_{0\theta}$. An advanced shooting method, first developed by Nishimura *et al* [13] for the finite β problem, has been adopted for this purpose. The algorithm involves numerical integration of the equation away from the singular layer towards the boundaries. The following analytic expressions representing asymptotic solutions for ψ near the resonant surface have been used to launch the numerical solutions:

$$\psi = A_l |s|^{h+1} - B_l |s|^{-h}; \quad \text{for } x < x_s, \quad (17)$$

$$\psi = A_r |s|^{h+1} + B_r |s|^{-h}; \quad \text{for } x > x_s, \quad (18)$$

where $x = r/r_s, r_s$ is the location of the singular layer and $s = x - x_s$.

$$h = -\frac{1}{2} + \frac{1}{2} \sqrt{1 - 4D_s}.$$

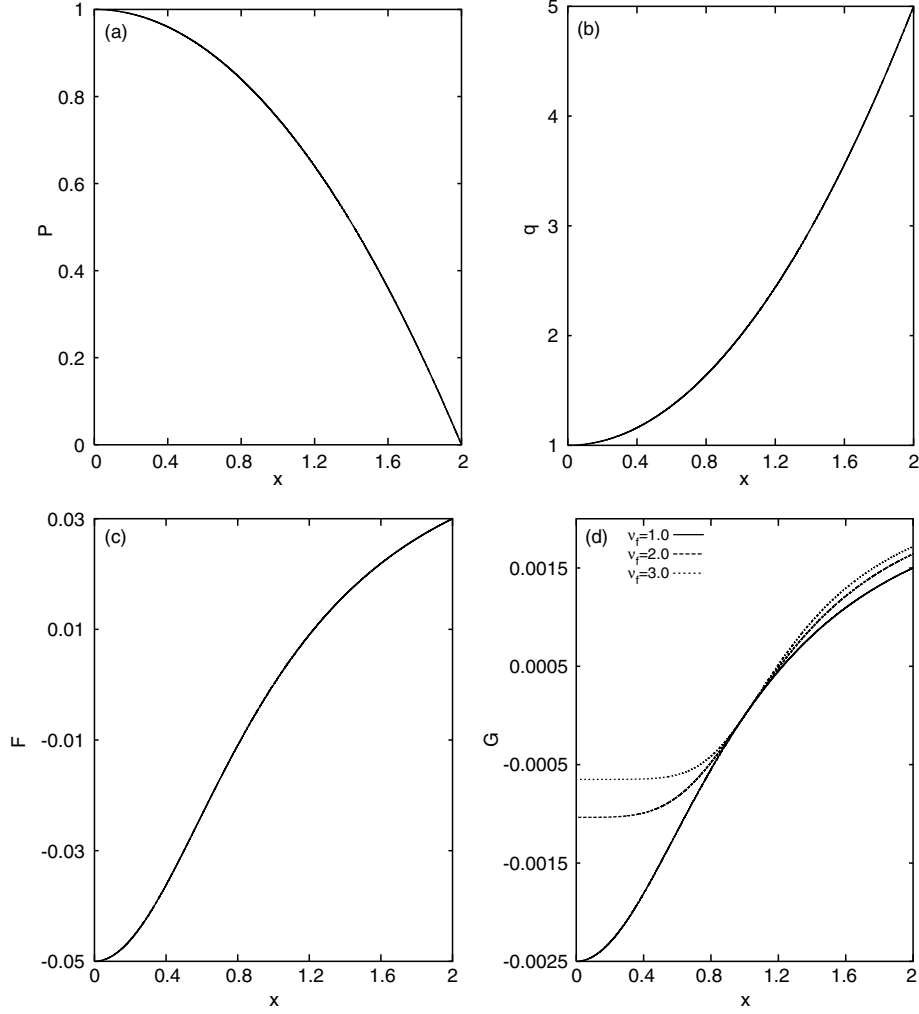


Figure 2. Profiles of (a) P (pressure), (b) q , (c) F and (d) G .

The Mercier coefficient D_s is given as

$$\begin{aligned}
 D_s = & -\frac{q_s^2}{q_s'^2 \alpha x_s} \left[\beta \frac{dP_0}{dx} + \frac{2x}{Hk_z^2 r_s^2} V_{0\theta} \frac{dV_{0\theta}}{dx} + \frac{2}{Hk_z^2 r_s^2} \right. \\
 & \times \left(\frac{m^2}{k_z^2 r_s^2 x^2 + m^2} - \frac{2}{\alpha} \right) V_{0\theta}^2 + \left(\frac{4G}{\alpha F} \frac{B_{0\theta}}{x} - \frac{2m}{\alpha x k_z^2 r_s} \frac{dG}{dx} \right) \\
 & \times \left(V_{0\theta} - \frac{G}{F} B_{0\theta} \right) - \frac{2m}{\alpha x k_z^2 r_s} \frac{G}{F} \left(\frac{dG}{dx} + \frac{2mV_{0\theta}}{r_s x^2} \right) \\
 & \left. \times \left(B_{0\theta} - \frac{G}{F} V_{0\theta} \right) + \frac{4}{\alpha Hk_z^2 r_s^2} \frac{G}{F} V_{0\theta} B_{0\theta} \right]_{x=x_s}. \quad (19)
 \end{aligned}$$

We iterate the constants A and B until the solution satisfies the appropriate boundary conditions [13]. The value of Δ' is then obtained as

$$\Delta' = \frac{A_r}{B_r} - \frac{A_l}{B_l}.$$

In the absence of flow our numerical values of Δ' agree with those of Nishimura *et al* [13] for a choice of their model profile.

4. Results and discussion

We now present our numerical results of Δ' values obtained for the $(m = 2, n = 1)$ tearing mode. We have used the following equilibrium profile for the normalized poloidal magnetic field

$$B_{0\theta}(x) = \frac{r_s}{Rq_0} \frac{x}{(1+x^{2\nu})^{1/\nu}}; \quad q(x) = q_0(1+x^{2\nu})^{1/\nu},$$

where R the major radius is taken to be a constant quantity and ν is an index that controls the flatness of the magnetic profile. To account for finite β effects we have chosen the normalized pressure profile to be

$$P_0(x) = 1 - \left(\frac{x}{x_b} \right)^2.$$

The equilibrium pressure balance is ensured by providing a small variation in B_{0z} . The plasma boundary is chosen to be at $x_b = 2$ and by constructing $x_s = 1$. Note that since $q(x_s) = m/n = 2$, for the $(2, 1)$ tearing mode, the index ν and the quantity q_0 are related as $q_0 = 2^{1-(1/\nu)}$. For the velocity profile we have chosen the following model form,

$$V_{0\theta}(x) = \frac{r_s V_{0z}}{Rq_{v0}} \frac{x}{(1+x^{2\nu_f})^{1/\nu_f}}; \quad q_v(x) = q_{v0}(1+x^{2\nu_f})^{1/\nu_f},$$

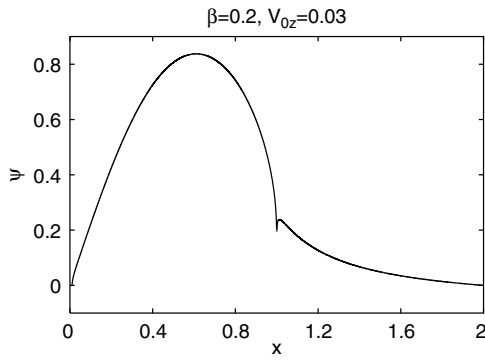


Figure 3. Eigenfunction ψ for the $(m = 2, n = 1)$ mode.

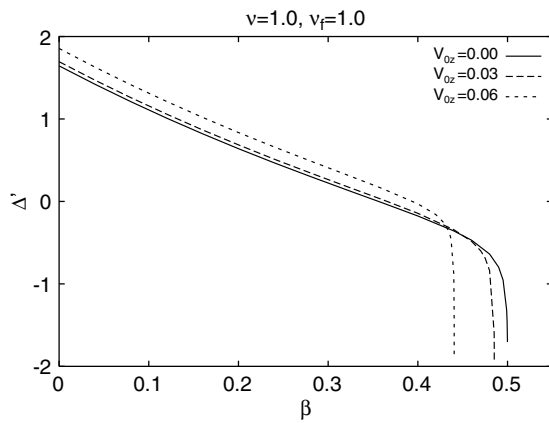


Figure 4. Change of Δ' with β for different V_{0z} .

where $q_v = r V_{0z}/(R V_{0\theta})$. For our numerical studies we have chosen V_{0z} to be constant corresponding to differential flow at the core with respect to the edge and used a profile in $V_{0\theta}$ whose peakedness is controlled by the index ν_f . For convenience we choose $q_{v0} = m/2^{(1/\nu_f)}$ which makes the magnetic and velocity profiles to have a similar behaviour near the singular layer, i.e. $G = 0$ where $F = 0$. Such a choice does not pose a serious physical restriction on the choice of velocity profiles since G has been defined in a rotating frame and the velocity profile in the laboratory frame (namely, \tilde{G}) is allowed to vanish at a place other than where $F = 0$. Our present choice makes the numerical analysis a lot easier and does not change the overall stability results. Figure 1 shows two sets of profiles of $B_{0\theta}$ and $V_{0\theta}$ plotted for values of $(\nu = 1.0, 3.0)$ and $(\nu_f = 1.0, 3.0)$ respectively, and other typical equilibrium profiles are shown in figure 2. Figure 3 depicts a typical eigenfunction for the $(m = 2, n = 1)$ mode. In figure 4 we have plotted the variation of Δ' with β for various values of the flow velocity V_{0z} . The flatness profile indices ν and ν_f are held constant at the value of unity. The solid curve (no flow case) corresponds to the previous result of Nishimura *et al* [13] and shows the stabilizing effect of finite β on Δ' . Due to a factor of 2 difference in the definition of β between our normalization and that adopted in [13], the x axis scale is expanded by a factor of 2 in our case. When finite flow velocity is turned on (at the same values of ν and ν_f) we notice two differences from the no flow result. At low β finite flow has a slightly destabilizing effect but the threshold β at which the curve begins to sharply drop to negative values is decreased as seen from the two other

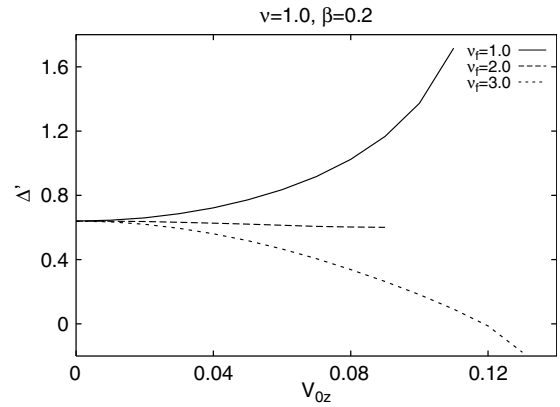


Figure 5. Change of Δ' with V_{0z} for different $V_{0\theta}$ profiles.

curves in the figure. Thus one can access higher β values more easily in the presence of flows. This trend however is strongly influenced by the shape of the velocity profile. This is shown in figure 5 where the variation of Δ' with V_{0z} is shown at a fixed value of $\beta = 0.2$, $\nu = 1$ and for different values of ν_f . As ν_f increases we see that there is a change in the behaviour of Δ' beyond a threshold value of ν_f and flow begins to have a stabilizing effect. This sensitivity to the profile parameter is also seen for the magnetic field. In figure 6 we show how Δ' changes with the magnetic field flatness parameter ν for a zero β plasma. As can be seen there is a dramatic rise in the value of Δ' as ν increases, i.e. as the magnetic field profile gets more peaked. At a given value of ν if ν_f is raised then Δ' decreases somewhat indicating that raising the peakedness of the flow profile has a stabilizing influence. The stabilizing influence is more pronounced at higher values of ν . We have also studied the effect of finite β on Δ' with velocity profiles of different ν_f and for a fixed value of $\nu = 1$. It is found that β has a stabilizing influence on Δ' at a given value of $\nu = 1$ in agreement with the results of [13]. Increasing ν_f at this value of ν and for a given value of β provides a further stabilizing influence but the incremental effect is small. However the trend changes distinctly when the value of ν is increased to higher values. As figure 7 demonstrates, for a value of ν exceeding a critical value increasing β can have a destabilizing effect (e.g. the curves for $\nu = 2, 3$ with $\nu_f = 2$). This is very similar to the turnover behaviour that is observed in figure 5 for the Δ' versus V_{0z} curve where ν_f is changed keeping β and ν constant.

5. Conclusions

These numerical results suggest that the combination of the magnetic and velocity profile variations along with finite β effects can profoundly influence the magnitude of Δ' and consequently the stability of the tearing mode. It should be mentioned here that in our present formulation we have not made an independent assessment of toroidal and poloidal flows on the stability of the mode. Our analysis is based on the variation of a quantity q_v which combines the ratio of these two velocities in a manner analogous to what the quantity q does in the case of the equilibrium magnetic fields. Thus the magnitude of the flow is represented by q_{v0} and the velocity shear is varied by changing the profile

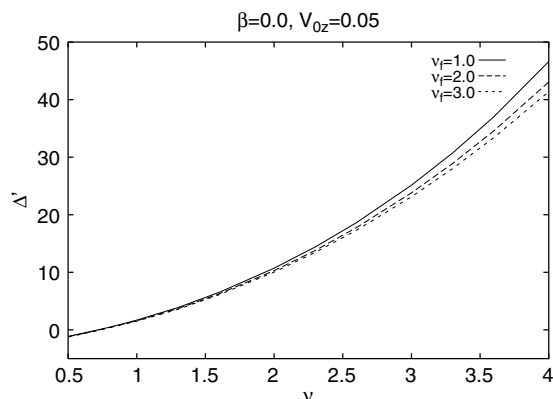


Figure 6. Change of Δ' with ν for different $V_{0\theta}$ profiles.

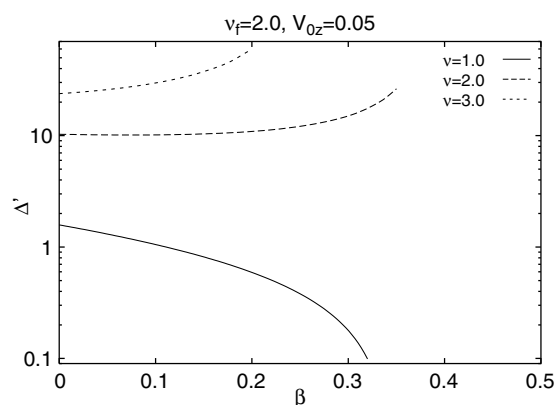


Figure 7. Change of Δ' with β for different $B_{0\theta}$ profiles.

index ν_f . The figures illustrating the numerical results reveal the dependence of Δ' on these quantities. This global dependence of Δ' needs to be appropriately accounted for when estimating stability thresholds or saturation widths of magnetic islands in the nonlinear Rutherford theory. Our outer layer equation (14) provides a means for estimating Δ' in the presence of sheared flows particularly for large

aspect ratio machines. When toroidal effects become important it is necessary to generalize the equation to account for the additional geometric effects. The toroidal outer layer equation will be similar to the cylindrical ones except for the presence of flux surface averaged metric element terms [13, 16]. Our present calculations were done with simple model profiles and in a limited parametric space to highlight the sensitivity of Δ' to the equilibrium profile parameters. A more direct utility of our equation would be to estimate Δ' using realistic equilibrium profiles obtained from MHD equilibrium codes. We are presently carrying out such a calculation using profiles from TOQ in order to get a better understanding of the stability results obtained from the NEAR code [10].

References

- [1] ITER Physics Expert Group on Disruptions, Plasma Control and MHD, ITER Physics Basis Editors 1999 *Nucl. Fusion* **39** 2251
- [2] Hegna C.C. 1998 *Phys. Plasmas* **5** 1767
- [3] Sovinec C.R., Gianakon T.A., Held E.D., Kruger S.E., Schnack D.D. and the NIMROD Team 2003 *Phys. Plasmas* **10** 1727
- [4] Hofmann I. 1975 *Plasma Phys.* **17** 143
- [5] Chen X.L. and Morrison P.J. 1990 *Phys. Fluids B* **2** 495
- [6] Chen X.L. and Morrison P.J. 1992 *Phys. Fluids B* **4** 845
- [7] Wessen K.P. and Persson M. 1991 *J. Plasma Phys.* **45** 267
- [8] Finn J.M. 1995 *Phys. Plasmas* **2** 198
- [9] Finn J.M. and Sovinec C.R. 1998 *Phys. Plasmas* **5** 461
- [10] Chandra D., Sen A., Kaw P., Bora M.P. and Kruger S. 2005 *Nucl. Fusion* **45** 524
- [11] Kruger S., Hegna C.C. and Callen J.D. 1998 *Phys. Plasmas* **5** 4169
- [12] Sen A., Chandra D., Kaw P., Bora M.P. and Kruger S. 2005 *32nd EPS Conf. Plasma Physics (Tarragona, 27 June–1 July 2005)* ECA vol 29C P-2.046
- [13] Nishimura Y., Callen J.D. and Hegna C.C. 1998 *Phys. Plasmas* **5** 4292
- [14] Lutjens H., Luciani J. and Garbet X. 2001 *Phys. Plasmas* **8** 4267
- [15] Furth H.P., Rutherford P.H. and Selberg H. 1973 *Phys. Fluids* **16** 1054
- [16] Hegna C.C. and Callen J.D. 1994 *Phys. Plasmas* **1** 2308